

# Simulation of 2D Free-surface Potential Flows Using a Robust Local Polynomial Collocation Method

Nan-Jing Wu<sup>1</sup>, \*Ting-Kuei Tsay<sup>2</sup>, Yang-Yih Chen<sup>1,3</sup>, and I-Chen Tsu<sup>2</sup>

<sup>1</sup> Tainan Hydraulics Laboratory, National Cheng Kung University, Tainan City 70955, Taiwan.

<sup>2</sup> Department of Civil Engineering, National Taiwan University, Taipei City 10617, Taiwan.

<sup>3</sup> Department of Marine Environment and Engineering, National Sun Yat-sen University, Kaohsiung City 80424, Taiwan.

\*Corresponding author: tktsay@ntu.edu.tw

## Abstract

In this paper a mesh-free numerical model for simulating 2D free-surface potential flows is established. A Lagrangian time-marching scheme is chosen for the boundary conditions of the moving and deforming free surface while a local polynomial collocation method is applied for solving the Laplace equation at each time step. The collocation method is developed in a way that the governing equation is satisfied on boundaries as well as boundary conditions. At any free surface node, this gives accurate estimation of the derivatives of velocity potential, which represent components of the velocity vector at that specific node. Therefore, trajectories of the free surface nodes can be predicted precisely. The numerical model is applied to the simulation of free surface waves in the liquid sloshing of a swaying tank. Present model is verified by comparing the numerical results with experimental data. Fairly good agreements are observed.

**Keywords:** mesh-free, collocation, sloshing, free surface waves

## Introduction

For several decades, water wave problems are treated as potential flow problems governed by the Laplace equation subjected to two nonlinear free surface boundary conditions. Due to the deformation of the free surface, mesh re-generation is needed if one uses a grid-based method to solve this kind of problems. Mesh generation, which means construction of the connectivity among the nodes, is a tedious task. Because the governing equation is the Laplace equation, the Boundary Element Method (BEM, also denominated as Boundary Integral Equation Method, BIEM) is mostly employed to this kind of problems. (Longuet-Higgins and Cokelet, 1976; Grilli et al., 1989; Ohyama and Nadaoka, 1991; Grilli and Watts, 1999; Grilli et al., 2001, 2002)

A mesh-free method, which is named as Method of Fundamental Solutions (MFS), was applied to solve the Laplace equation in the fully nonlinear water wave problems. (Wu et al., 2006, 2008; Wu and Tsay, 2009) When using MFS, one has to place source points outside the domain. Because the values of the fundamental solutions are just related to the distances from the source points, fundamental solutions could be regarded as a Radial Basis Functions (RBF). Collocation is only needed on the boundaries, so MFS is a boundary type RBF collocation method. Though MFS could be employed to fully nonlinear water wave problems, its applicability is still limited because numerical blow up might occur when the free surface approaches too close to the source points.

Wu and Chang (2011) proposed a modified RBF Collocation Method that guarantees the accurate estimation of partial derivatives of the velocity potential on the free surface. By integrating with a Lagrangian time-marching scheme, the trajectories of the free surface nodes can be precisely predicted. However, the full matrix formed in that method limits its applicability to large-scale problems.

Besides treating water wave flows as potential flows, one could also choose Navier-Stokes equation or Reynolds Averaged Navier-Stokes equation models, such as models using Arbitrary Lagrangian-

Eulerian method (ALE) (Lo and Young, 2004), Volume of Fluid method (VOF) (Lin and Liu, 2008), Smoothed Particle Hydrodynamics (SPH) (Li and Liu, 2002), and Moving Particle Semi-implicit method (MPS) (Hori et al., 2011). Models using ALE or VOF are grid-based while models using SPH or MPS are meshless ones. Results of these models are more close to the real flow. However, these models are more time consuming and computer memory storage consuming.

Wu and Tsay (2013) proposed a local polynomial collocation method for the purpose of solving general partial differential equations. This method originates from the Finite Point Method (FPM) of Oñate et al. (1996a, b). It is a localized meshless method thus matrix formed in the collocation process is very sparse. The collocation method was developed in a way that the governing equation as well as boundary conditions is satisfied on boundaries. This method is more robust than conventional collocation methods.

Adopting the time-marching scheme for the free surface proposed by Wu and Chang (2011), and the local polynomial collocation method proposed by Wu and Tsay (2013), a numerical model for the fully nonlinear free surface potential flow is developed. In this paper, it is employed to simulate motions of liquid sloshing in a swaying tank.

### Mathematical description for free-surface potential flow

For inviscid, incompressible fluids, the governing equation of free-surface potential flow is the Laplace equation.

$$\nabla^2 \phi = 0 \quad (1)$$

where  $\phi$  is the velocity potential and the relation between velocity and velocity potential is  $\bar{v} = \nabla \phi$ . On the free surface, kinematic and dynamic boundary conditions are to be satisfied.

$$\nabla \phi = \frac{d\bar{x}}{dt} \quad (2)$$

$$\left. \frac{d\phi}{dt} \right|_{z=\eta} = -gz + \frac{1}{2} \nabla \phi \cdot \nabla \phi \quad (3)$$

where  $\eta$  is the free surface displacement,  $g$  is the gravitational acceleration. Both of them have been transformed onto the Lagrangian aspect. The boundary condition at the water-structure interface is the no-flux boundary condition, which can be expressed as

$$\bar{n} \cdot \nabla \phi = \bar{n} \cdot \bar{v}_b \quad (4)$$

where  $\bar{n}$  is the unit normal vector outward from the domain, and  $\bar{v}_b$  is the velocity of the moving solid boundary.

### Time marching scheme in the numerical model

For solving this kind of time-dependent problems, the time domain firstly has to be discretized. At each time step, the Laplace equation needs to be solved once to obtain the velocity potential for the entire domain thus to further determine the velocity. Boundary positions are updated by the given motion of the solid boundaries and the prediction from the time marching process of the free-surface boundary. Wu and Chang (2011) employed the second order central difference to Eq. 3.

$$(\phi|_{\bar{x}=\bar{x}_j})^{(n)} = (\phi|_{\bar{x}=\bar{x}_j})^{(n-2)} + 2\Delta t \left[ \left( -gz + \frac{1}{2} \nabla \phi \cdot \nabla \phi \right)_{\bar{x}=\bar{x}_j} \right]^{(n-1)} \quad (5)$$

where  $\bar{x}_j$  denotes the position of the  $j^{\text{th}}$  node and this equation is only valid in case the node is on the free surface. In this formulation, the required data on the right-hand side for seeking the velocity potential in the entire domain at the  $n^{\text{th}}$  time step, including the nonlinear terms, are already known. What one needs to do first is just to determine the position of each traced ‘particle’,  $\bar{x}_j^{(n)}$ . It was proposed to use the second-order finite difference scheme in the time domain.

$$\bar{x}_j^{(n)} = \bar{x}_j^{(n-2)} + 2\Delta t (\nabla \phi|_{\bar{x}=\bar{x}_j})^{(n-1)} \quad (6)$$

Here it should be noted that this equation is valid for all the nodes. When the velocity potential for the entire domain is obtained, the velocity at each of the nodes can be estimated accurately. The Crank-Nicolson formula is then applied for better numerical stability.

$$\bar{x}_j^{(n)} = \bar{x}_j^{(n-1)} + \frac{\Delta t}{2} \left[ (\nabla \phi|_{\bar{x}=\bar{x}_j})^{(n)} + (\nabla \phi|_{\bar{x}=\bar{x}_j})^{(n-1)} \right] \quad (7)$$

Note that there is no need to solve the Laplace equation again because there is barely difference between the free-surface velocity potential at  $\bar{x}_j^{(n)}$  predicted by using Eq. 6 and that predicted by using Eq. 7.

### Method for solving the Laplace equation

At each time step, the Laplace equation needs to be solved once. There are many methods for solving the Laplace equation numerically, either grid-based or mesh-free. In this study the local polynomial collocation method proposed by Wu and Tsay (2013) is chosen. It is a mesh-free method for solving general partial differential equations. It is so chosen to accommodate efficiently the deformation of the free surface boundary. Following gives a brief description of this meshless numerical method.

When solving a general 2-D linear second order PDE as

$$\mathcal{L}\{\phi\} = c_1 \phi + c_2 \frac{\partial \phi}{\partial x} + c_3 \frac{\partial \phi}{\partial y} + c_4 \frac{\partial^2 \phi}{\partial x^2} + c_5 \frac{\partial^2 \phi}{\partial y^2} + c_6 \frac{\partial^2 \phi}{\partial x \partial y} = s \quad (8)$$

subjected to the boundary conditions

$$\mathcal{B}\{\phi\} = q_1 \phi + q_2 \frac{\partial \phi}{\partial x} + q_3 \frac{\partial \phi}{\partial y} = f, \quad \bar{x} \in \Gamma_1 \quad (9)$$

$$\phi = \phi_b, \quad \bar{x} \in \Gamma_2 \quad (10)$$

where  $c_1, c_2, \dots, c_6, q_1, q_2, q_3, f$  and  $s$  are all functions of  $x$  and  $y$ . The boundary  $\Gamma_1$  could be non-smooth and then at a corner there could be more than one Robin condition. Therefore,  $q_1, q_2, q_3$ , and  $f$  could be multi-valued. Boundary condition can be expressed just as Eq. 9 for conciseness. It will be explained later on how boundary conditions will be treated at a point where more than one boundary condition exists. In seeking the numerical solutions, the entire domain is distributed with  $N$  nodes as needed. At each node,  $\phi$  is approximated as

$$\phi(\bar{x})|_{\bar{x} \approx \bar{x}_j} \approx \hat{\phi}_j(\bar{x}) = \sum_{i=1}^m \alpha_{ji} p_i(\bar{X}) \quad (11)$$

in which  $\bar{X} = \bar{x} - \bar{x}_j$  is the relative position vector,  $p_i(\bar{X})$  is the  $i^{\text{th}}$  monomial of the polynomial, and  $\alpha_{ji}$  are coefficients to be determined. The subscript  $j$  indicates that this approximation is valid only in the vicinity of  $\bar{x}_j$ . Once a new  $\bar{x}_j$  is chosen, there will be a new set of  $\alpha_{ji}$ . For a 2-D problem, the monomials are

$$\{p_i(\bar{X}), i=1 \sim m\} = \{1 \quad X \quad Y \quad X^2 \quad Y^2 \quad XY \quad \dots\} \quad (12)$$

in which  $\bar{X} = X \bar{i} + Y \bar{j}$ . The value of  $m$  is related to the chosen degree of the polynomial. Here the error residual of the local approximation around  $\bar{x} = \bar{x}_j$  is defined as

$$E_j = \sum_{l=1}^N \left( W_{jl} \left( \phi(\bar{x}_l) - \hat{\phi}_j(\bar{x}_l) \right)^2 \right) \quad (13)$$

where  $W_{jl}$  is a weighting factor determined by the distance between  $\bar{x}_j$  and  $\bar{x}_l$ . Usually, the normalized Gaussian function is selected for determining the weighting factor

$$W_{jl} = \begin{cases} \frac{\exp(-\varepsilon(r_{jl} / \rho_j)^2) - \exp(-\varepsilon)}{1 - \exp(-\varepsilon)} & , r_{jl} < \rho_j \\ 0 & , r_{jl} \geq \rho_j \end{cases} \quad (14)$$

where  $r_{jl}$  is the distance between  $\bar{x}_j$  and  $\bar{x}_l$  (i.e.  $r_{jl} = |\bar{x}_l - \bar{x}_j|$ ),  $\varepsilon$  is the shape parameter, and  $\rho_j$  is the supporting range measured from the point of  $\bar{x}_j$ . Considering only the non-zero terms, Eq. 13 can be rewritten as

$$E_j = \sum_{k=1}^n \left( W_{jk} \left( \phi(\bar{x}_k) - \hat{\phi}_j(\bar{x}_k) \right)^2 \right) \quad (15)$$

where  $k$  is the local index of  $\bar{x}_l$  in the  $j^{\text{th}}$  sub-domain and  $n$  is number of nodes inside the sub-domain. The coefficients of the local polynomial corresponding to the minimal error residual at the node  $\bar{x}_j$  under the condition that

$$\left( \mathcal{L}\{\phi\} - s \right)^2 + \left( \mathcal{B}_1\{\phi\} - f_1 \right)^2 + \dots + \left( \mathcal{B}_{n_{nd}}\{\phi\} - f_{n_{nd}} \right)^2 \rightarrow 0 \quad (16)$$

where  $n_{nd}$  is the number of non-Dirichlet boundary conditions at the node  $\bar{x} = \bar{x}_j$ , can be expresses as

$$[\alpha_j] = [\Lambda] \begin{bmatrix} \beta \\ \beta' \end{bmatrix} \quad (17)$$

in which

$$[\Lambda]_{m \times (n+n_{nd}+1)} = \left( \begin{bmatrix} A \\ A' \end{bmatrix}^T \begin{bmatrix} A \\ A' \end{bmatrix} \right)^{-1} \begin{bmatrix} A \\ A' \end{bmatrix}^T \quad (18)$$

$$[A]_{n \times m} = \begin{bmatrix} a_{11} & a_{12} & \cdots & \cdots & a_{1m} \\ a_{21} & \ddots & & & a_{2m} \\ \vdots & & a_{ki} & & \vdots \\ \vdots & & & \ddots & \vdots \\ a_{n1} & a_{n2} & \cdots & \cdots & a_{nm} \end{bmatrix} \quad (19)$$

$$[A']_{(n_{nd}+1) \times m} = \begin{bmatrix} w'c_1 & \cdots & \cdots & \cdots & w'c_p & 0 & \cdots & 0 \\ w'q_{1,1} & \cdots & w'q_{1,3} & 0 & \cdots & \cdots & \cdots & 0 \\ \vdots & & \vdots & \vdots & & & & \vdots \\ w'q_{n_{nd},1} & \cdots & w'q_{n_{nd},3} & 0 & \cdots & \cdots & \cdots & 0 \end{bmatrix} \quad (20)$$

$$[\beta]_{n \times 1} = [w_1\phi_1 \quad \cdots \quad w_k\phi_k \quad \cdots \quad w_n\phi_n]^T \quad (21)$$

$$[\beta']_{(n_{nd}+1) \times 1} = [w's \quad w'f_1 \quad \cdots \quad w'f_{n_{nd}}]^T \quad (22)$$

where  $w_k = \sqrt{W_{jk}}$ ,  $\phi_k = \phi(\bar{x}_k)$ ,  $a_{ki} = w_k p_i(\bar{x}_k - \bar{x}_j)$ , and  $w' = \sqrt{W'}$ . In case of  $n_{nd}$  in Eq. 16 is greater than 1, it obviously indicates that the collocation point rests on an edge or at a corner. At an internal node, there is only one term in Eq. 16 (i.e.  $n_{nd} = 0$ ). The symbol  $W'$  represents a penalty weighting factor whose value is much greater than 1. Assembling the local approximations into a global matrix system, one gets

$$[K]_{N \times N} [\phi]_{N \times 1} = [b]_{N \times 1} \quad (23)$$

In case that the value of  $\phi$  is known at  $\bar{x}_j$ , the entities in Eq. 23 are

$$\kappa_{jl} = \begin{cases} 1, & \text{if } j=l \\ 0, & \text{otherwise} \end{cases} \quad (24)$$

$$b_j = \phi_j \quad (25)$$

Otherwise,

$$\kappa_{jl} = \begin{cases} w_k \lambda'_{1k} - \delta_j(l), & \text{if } |\bar{x}_j - \bar{x}_l| < \rho_j \\ 0, & \text{otherwise} \end{cases} \quad (26)$$

$$\delta_j(l) = \begin{cases} 1, & \text{if } j=l \\ 0, & \text{otherwise} \end{cases} \quad (27)$$

$$b_j = - \sum_{k=1}^{n_{nd}+1} \lambda'_{1,(n+k)} \beta'_k \quad (28)$$

It should be noted that the symbol  $k$  in Eqs. 19, 21, 26 and 28 is the local index of  $\bar{x}_i$  in the  $j^{\text{th}}$  sub-domain. The approximated partial derivatives of the solution, which are related to the coefficients of the local polynomial approximation, can then be determined by

$$\begin{aligned} \phi|_{\bar{x}=\bar{x}_j} &\approx \hat{\phi}|_{\bar{x}=\bar{x}_j} = \alpha_{j1}, \quad \frac{\partial \phi}{\partial x}|_{\bar{x}=\bar{x}_j} \approx \frac{\partial \hat{\phi}}{\partial x}|_{\bar{x}=\bar{x}_j} = \alpha_{j2}, \quad \frac{\partial \phi}{\partial y}|_{\bar{x}=\bar{x}_j} \approx \frac{\partial \hat{\phi}}{\partial y}|_{\bar{x}=\bar{x}_j} = \alpha_{j3}, \quad \frac{\partial^2 \phi}{\partial x^2}|_{\bar{x}=\bar{x}_j} \approx \frac{\partial^2 \hat{\phi}}{\partial x^2}|_{\bar{x}=\bar{x}_j} = 2\alpha_{j4}, \\ \frac{\partial^2 \phi}{\partial y^2}|_{\bar{x}=\bar{x}_j} &\approx \frac{\partial^2 \hat{\phi}}{\partial y^2}|_{\bar{x}=\bar{x}_j} = 2\alpha_{j5}, \quad \frac{\partial^2 \phi}{\partial x \partial y}|_{\bar{x}=\bar{x}_j} \approx \frac{\partial^2 \hat{\phi}}{\partial x \partial y}|_{\bar{x}=\bar{x}_j} = \alpha_{j6}, \dots \end{aligned} \quad (29)$$

The shape parameter  $\varepsilon$  in the normalized Gaussian function has been shown to be insensitive by Wu and Tsay (2013). Analyses of the convergence rate of nodal resolution were also carried out by Wu and Tsay (2013) while related analysis of nodal arrangement has been done by Wu et al (2013). The suggestions of Wu and Tsay (2013) for choosing the values of the shape parameter  $\varepsilon$ , the sub-domain size  $\rho_j$ , the penalty weighting factor  $W'$  are followed. Therefore, in this study,  $\varepsilon = 22$ ,  $\rho_j$  equal to 1.05 times of the distance from  $\bar{x}_j$  to its 25<sup>th</sup> nearest neighboring node, and  $W' = 10^4$  are used in all numerical computations.

## Applications and Verifications

### *Description of the test problem*

For testing their numerical model, Liu and Lin (2008) carried out a sloshing experiment. The layout of the experiment is shown in Figure 1. The non-breaking case with the strongest nonlinear effect in the experiment is chosen as the verification of present model. The period of the oscillation is 1.0372 sec. The amplitude of the oscillation is 0.5 cm.

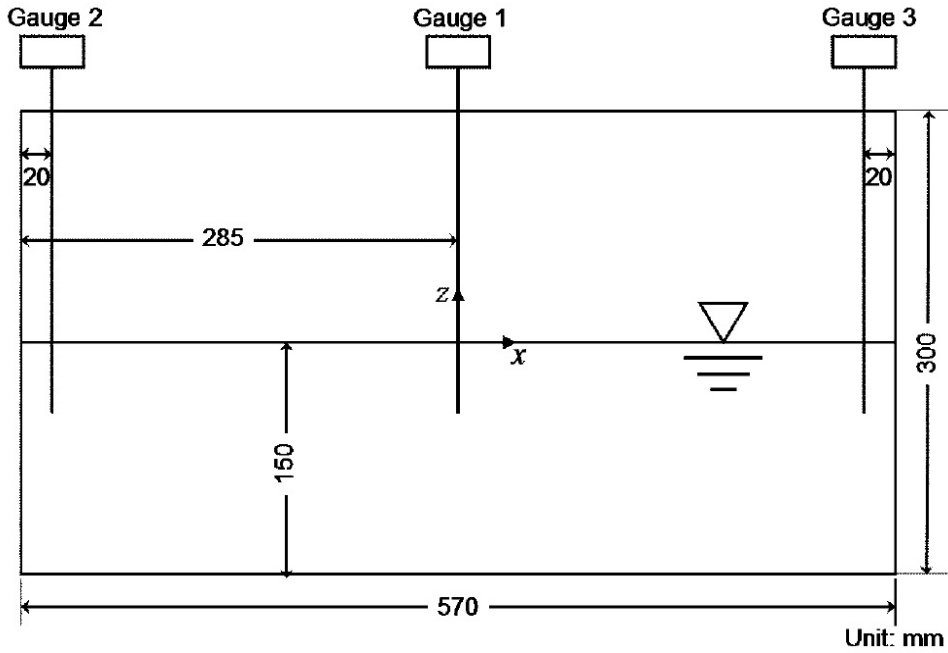


**Figure 1. Layout of the sloshing experiment of Liu and Lin (2008)**

### *Model setup*

Discretizing a wave length with at least 20 segments, the initial nodal spacing on the free surface is chose as 5.18 cm. The collocation points are initially distributed as a hexagonal close packing array so that the most compact nodal arrangement can be achieved. Therefore, the vertical nodal spacing on the side walls is 3 cm. Totally, there are 127 collocation points. The time step chosen in the simulation is 1/80 of the swaying period. The initial nodal distribution is shown in Figure 2.

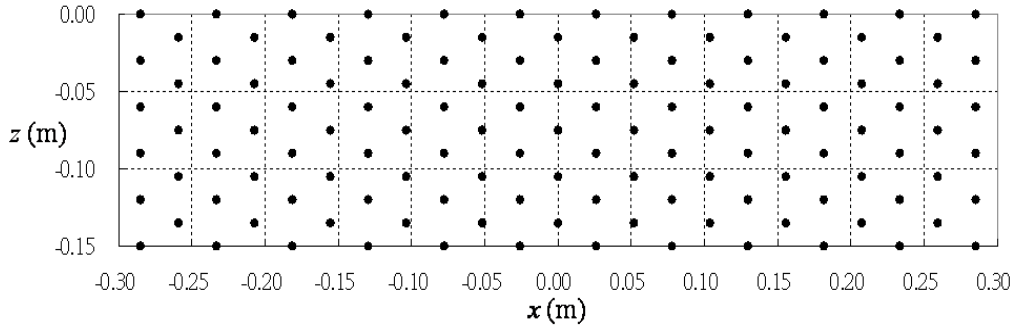
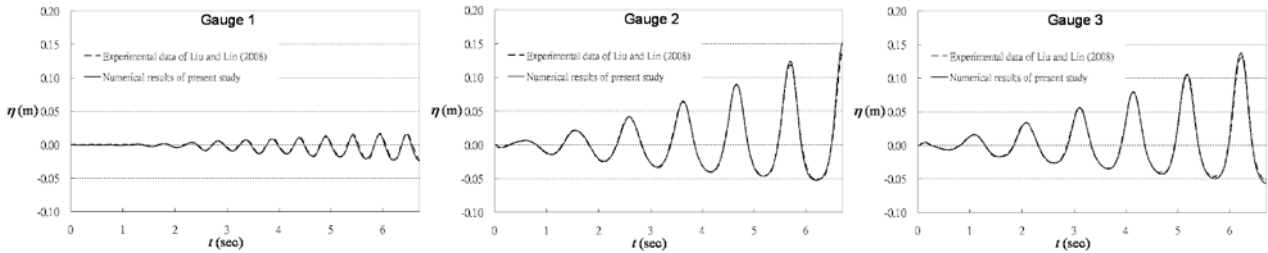


**Figure 2. Initial nodal distribution of the numerical model**

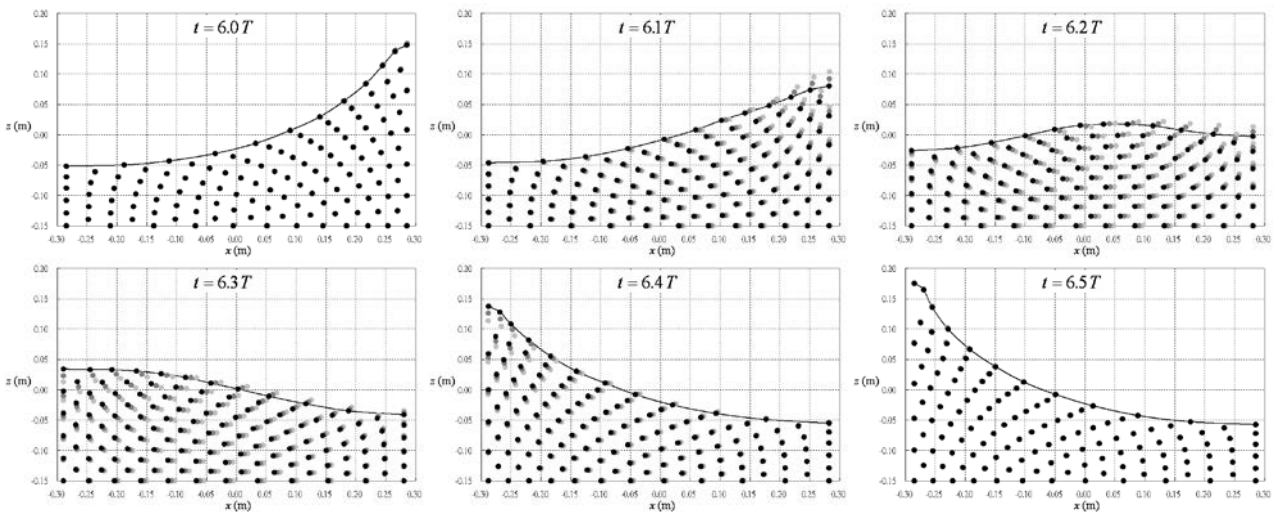
### Numerical results

Figure 3 shows the comparison of the numerical results with the experimental data. Very good agreement is found. It is also found that the higher the peak grows, the flatter the trough becomes. This indicates an increase of nonlinear effect as the tank oscillation continues. In the simulation the side walls are set to be infinitely high but in the experiment the tops of the two side walls are just 15 cm high from the still water level. It had not been mentioned in the paper of Liu and Lin (2008) what happened when the free surface elevation goes higher than the height of side walls. In present simulation, free surface elevation goes over the top of the right side wall at  $t = 6.184$  sec. This might be the reason why the simulated  $\eta$  in the last wave period are slightly higher than observed.

Figure 4 shows the positions of the traced fluid particles in the time interval of  $t = 6.0T \sim 6.5T$ . This figure shows that at the end of simulation, the run-up becomes much higher than the initial water depth. It is an indication of very strong nonlinearity on the free surface.



**Figure 3. Comparison of the numerical results with the experimental data**



**Figure 4. Snapshots of traced fluid particles in the time interval of  $t = 6.0T \sim 6.5T$**

Only 9 seconds is needed to simulate this case by using just one processing unit of Intel(R) Core™ i7-3370 CPU. The nodal spacing of present model is an order larger than the grid size in the model of Liu and Lin (2008). Present model is much more efficient in this case.

## Conclusions

A numerical model is presented in this paper by treating water wave phenomenon as potential flow of fluid motion with a free surface. The problem is governed by the Laplace equation and subjected to nonlinear free surface boundary conditions. The free surface boundary conditions are discretized by using the Lagrangian time-marching scheme of Wu and Chang (2011) so that Laplace equation is only required to be solved numerically once at each time step. The method chosen for solving the Laplace equation is the local polynomial collocation method proposed by Wu and Tsay (2013). Present model is applied to the simulations of liquid sloshing in a swaying tank. It is much more efficient in a testing problem because CPU time of the simulation takes only seconds. Fairly good agreement is found in the comparison with experimental data.

## Acknowledgement

The authors acknowledge the National Science Council of Taiwan for financial support (grant numbers: NSC 102-2911-I-006-302 and NSC 102-2221-E-002-155).

## References

- Grilli S.T., Skourup J., and Svendsen I.A. (1989), An efficient boundary element method for nonlinear water waves. *Engineering Analysis with Boundary Elements* 6, pp. 97–107.
- Grilli S.T. and Watts P. (1999), Modeling of waves generated by a moving submerged body. Applications to underwater landslides. *Engineering Analysis with Boundary Elements*, 23, pp. 645–656.
- Grilli S.T., Guyenne P., and Dias F. (2001), A fully nonlinear model for three-dimensional overturning waves over an arbitrary bottom. *International Journal for Numerical Methods in Fluids* 35, pp. 829 – 867.
- Grilli S.T., Vogelmann S., and Watts, P. (2002), Development of a 3d numerical wave tank for modeling tsunami generation by underwater landslides. *Engineering Analysis with Boundary Elements* 26, pp. 301-313.
- Hori C., Gotoh H., Ikari H., and Khayyer A. (2011), GPU-acceleration for Moving Particle Semi-Implicit Method. *Computers and Fluids* 51, pp. 174-183.
- Li S.F. and Liu W.K. (2002), Meshfree and particle methods and their applications. *Appl Mech Rev* 55, pp. 1-34.
- Liu D. and Lin P. (2008), A numerical study of three-dimensional liquid sloshing in tanks. *Journal of Computational Physics* 227, pp. 3921–3939.
- Lo D.C. and Young, D.L. (2004), Arbitrary Lagrangian–Eulerian finite element analysis of free surface flow using a velocity–vorticity formulation. *Journal of Computational Physics* 195, pp. 175 –201.
- Longuet-Higgins H.S. and Cokelet E.D. (1976), The deformation of steep waves on water, I, a numerical method of computation. *Proc R Soc Lond A* 350, pp. 1–26.
- Ohya T. and Nadaoka K. (1991), Development of a numerical wave tank for analysis of nonlinear and irregular wave field. *Fluid Dynamic Research* 8, pp. 231–251.
- Oñate E., Idelsohn S., Zienkiewicz O.C., and Taylor R.L. (1996), A finite point method in computational mechanics. Applications to convective transport and fluid flow. *International Journal for Numerical Methods in Engineering* 39, pp. 3839–3866.
- Oñate E., Idelsohn S., Zienkiewicz O.C., Taylor R.L., and Sacco C. (1996), A stabilized finite point method for analysis of fluid mechanics problems. *Computer Methods in Applied Mechanics and Engineering* 139, pp. 315–346.
- Wu N.J., Tsay T.K., and Young D.L. (2006), Meshless simulation for fully nonlinear water waves. *International Journal for Numerical Methods in Fluids* 50, pp. 219–234.
- Wu N.J., Tsay T.K., and Young, D.L. (2008), Computation of nonlinear free-surface flows by a meshless numerical method. *Journal of Waterway, Port, Coastal and Ocean Engineering* 134, pp. 97–103.
- Wu N.J. and Tsay T.K. (2009), Applicability of the method of fundamental solutions to 3-D wave–body interaction with fully nonlinear free surface. *Journal of Engineering Mathematics* 63, pp. 61–78.
- Wu N.J. and Chang, K.A. (2011), Simulation of free-surface waves in liquid sloshing using a domain-type meshless method. *International Journal for Numerical Methods in Fluids* 67, pp. 269-288.
- Wu N.J. and Tsay T.K. (2013), A robust local polynomial collocation method. *International Journal for Numerical Methods in Engineering* 93, pp. 355-375.
- Wu N.J., Tsay T.K., Yang T.C., and Chang H.Y. (2013), Orthogonal grid generation of an irregular region using a local polynomial collocation method, *Journal of Computational Physics* 243, pp. 58–73.